Remote sensing satellite's attitude control system: rapid performance sizing for passive scan imaging mode

Amirreza Kosari
Faculty of New Sciences and Technologies, University of Tehran, Tehran, Iran
Alireza Sharifi
Department of Surveying Engineering, Faculty of Civil Engineering, Shahid Rajaee Teacher Training University, Tehran, Iran
Alireza Ahmadi
Faculty of New Sciences and Technologies, University of Tehran, Tehran, Iran, and
Masoud Khoshsima
Satellite Research Institute, Iranian Space Research Center, Tehran, Iran

Abstract

Purpose – Attitude determination and control subsystem (ADCS) is a vital part of earth observation satellites (EO-Satellites) that governs the satellite's rotational motion and pointing. In designing such a complicated sub-system, many parameters including mission, system and performance requirements (PRs), as well as system design parameters (DPs), should be considered. Design cycles which prolong the time-duration and consequently increase the cost of the design process are due to the dependence of these parameters to each other. This paper aims to describe a rapid-sizing method based on the design for performance strategy, which could minimize the design cycles imposed by conventional methods.

Design/methodology/approach – The proposed technique is an adaptation from that used in the aircraft industries for aircraft design and provides a ball-park figure with little engineering man-hours. The authors have shown how such a design technique could be generalized to cover the EO-satellites platform ADCS. The authors divided the system requirements into five categories, including maneuverability, agility, accuracy, stability and durability. These requirements have been formulated as functions of spatial resolution that is the highest level of EO-missions PRs. To size, the ADCS main components, parametric characteristics of the matching diagram were determined by means of the design drivers.

Findings – Integrating the design boundaries based on the PRs in critical phases of the mission allowed selecting the best point in the design space as the baseline design with only two iterations. The ADCS of an operational agile EO-satellite is sized using the proposed method. The results show that the proposed method can significantly reduce the complexity and time duration of the performance sizing process of ADCS in EO-satellites with an acceptable level of accuracy.

Originality/value – Rapid performance sizing of EO-satellites ADCS using matching diagram technique and consequently, a drastic reduction in design time via minimization of design cycles makes this study novel and represents a valuable contribution in this field.

Keywords Very high resolution, Passive scan agile earth observation satellite, Attitude determination and control subsystem, Performance sizing, Requirements engineering, Imaging payload, Matching diagram technique

Paper type Research paper

Acronyms and abbreviations

2D	= 2-dimensional;
ACA	= Attitude Control Actuator;
ADCS	= Attitude Determination and Control;
ADS	= Attitude Determination Sensor;
AEOS	= Agile Earth Observation Satellite;
A-GLA	= Absolute-GeoLocation Accuracy;
COTS	= Commercial Of-The-Shelf;
DD	= Design Driver;
DEM	= Digital Elevation Model;
DP	= Design Parameter;
EO-Satellite	= Earth Observation Satellite;
FMC	= Forward Motion Compensation;
GLA	= GeoLocation Accuracy;
GSD	= Ground Sample Distance;
HR	= High Resolution;
IFOV	= Instant Field Of View;
IPL	= Imagining PayLoad;
KA	= Knowledge Accuracy;
LEOP	= Launch and Early Orbit Phase;
LR	= Low Resolution;
MDP	= Main Design Parameter;
MR	= Mid Resolution;

The current issue and full text archive of this journal is available on Emerald Insight at: **https://www.emerald.com/insight/1748-8842.htm**

Aircraft Engineering and Aerospace Technology
92/7 (2020) 1073–1083
 [ISSN 1748-8842]
[DOI 10.1108/AEAT-02-2020-0030]

Received 12 March 2020
Revised 1 May 2020
Accepted 7 May 2020

MT = Magnetic Torquer;
No. = Number of;
PA = Pointing Accuracy;
PR = Performance Requirement;
PS-AEOS = Passive Scan Agile Earth Observation Satellite;
R-GLA = Relative-GeoLocation Accuracy;
RW = Reaction Wheel;
SWaP = Size, Weight and Power;
TRL = Technology Readiness Level;
VHR = Very High Resolution; and
ZMB = Zero Momentum Bias.

1. Introduction

During space flight, a craft's attitude must be determined and controlled for reasons dependent upon its mission. Sensing equipment that is fixed into position, need to be aimed by slewing the craft; keeping its high gain antenna-oriented toward the earth for sending and receiving data and commands; keeping their solar arrays angled toward the sun to optimize power absorption and reduce the craft's reliance on internal power systems (Li *et al.*, 2017); thermal heating and cooling of the craft and its subsystems can also be controlled by the craft's orientation. Each one of these tasks imposes performance requirements (PRs) to design a custom attitude determination and control subsystem (ADCS) for an earth observation satellite (EO-satellite).

The proper performance of ADCS is assessed by its support for the imaging payload (IPL) to provide the required data, needed for producing remote sensing images. Performance is a general term that refers to the overall characteristics of ADCS and makes it attractive to be used in agile earth observation satellite (AEOS) platforms. The first and the most critical step in the ADCS design process is requirements engineering that means translation of high-levels into lower-level requirements (Palacios and Smith, 2019). The IPL PRs are at the highest level of priority, and the intermediate and lower-level requirements should be extracted from them.

In small satellites systematic design software, to size the EO-satellites' IPL, the PRs including spatial, spectral, radiometric and temporal resolutions should be input into the software by users. The users must also enter the input data, including "pointing accuracy" and "attitude control type" separately to size the custom ADCS (Kwiek, 2019). While, due to the dependence of IPL and ADCS performance to each other, the ADCS performance parameters could be determined by specifying the proper values to IPL ones. This approach reduces the time duration and, as a result, the cost of EO-satellites design. Although in some EO-missions, spatial and temporal resolutions considered as two crucial PRs but their relation to the ADCS design parameters (DPs) has not been defined clearly.

In the design process of the EO-satellites platform, ADCS could be designed knowing the "pointing accuracy" and "stability to an accuracy" (Xiong and Wei, 2017). Achieving these performance parameters via translation of higher-level requirements will make it possible to bargain on their values (Xie *et al.*, 2018). The stringent requirements can be modified by negotiating through the requirements engineering process and thereby reducing the cost and duration of the design process.

Due to the complexities involved in ADCS design, some efforts have been made to develop simpler algorithms (Akbaritabar *et al.*, 2018; Sun *et al.*, 2018). When the EO-mission requires to design and manufacture a custom ADCS (Tayebi *et al.*, 2017; Hua *et al.*, 2018) then the "design for performance" strategy can be one of the shortest ways to meet the PRs by determining the best values for ADCS DPs (Jia *et al.*, 2019). The matching diagram technique, as a tool in "design for performance" strategy, could be used to minimize the cycles of the ADCS design that leads to reduce the design process time and, ultimately, a reduction in the lifecycle cost of the EO-satellites. The proposed technique is a modification to that used in the aircraft industries (Laurence and Loftin, 1980) and aircraft design process (Torenbeek, 1976; Sadraey, 2013), and, provides a ball-park figure with little engineering man-hours (Roskam, 1985; Raymer, 1992).

This work consists of two parts. In the first section, the matching diagram technique has been generalized as a design tool and in the second section, the developed technique has been applied to performance sizing of an operational agile EO-satellite ADCS as a case, to demonstrate the effectiveness of the method.

2. Satellite Design strategy, general approach

Design strategy refers to the general framework that embodies pivot features in all phases of the system design. The pivot feature, itself, acts as the key driver for all decisions and selections (Wassan, 2006). "Design for performance" strategy, therefore, aims to reach a particular configuration; while knowing the system performance objectives. In other words, it is a process in which the system PRs must lead to the determination of boundary values for main design parameters (MDPs), which have the most significant impact on system behavior (Torenbeek, 1976). In this approach, we map all design constraints and requirements onto a certain two-dimensional space to facilitate the selection of the baseline design, which must represent a compromise among desirability, affordability and availability. Here, we apply such a technique to the ADCS. For that purpose, we need to somehow correlate performance parameters to the so-called physical DPs, considering two sets of principles as follows:

1. PRs could be directly extracted from available scientific rules and standard practices of the related fields or indirectly from mission and system requirements.
2. Design drivers (DDs), which determine the matching diagram parametric characteristics, are two arbitrary combinations of the MDPs, which are independent of the other DPs, controllable as needed and, have a direct impact on the system performance.

It is noted that the above principles are in line with the so-called axiomatic design practice (Malaek *et al.*, 2015).

2.1 Matching diagram, the design tool

With the help of the tools above, we could construct a specific frame of reference to exhibit ADCS characteristics together with its PRs. Such a frame of reference could help us compare the consequences of any decision related to the ADCS. With

the general procedure outlined in reference (Ahmadi *et al.*, 2018), the following steps, which schematically has been illustrated in Figure 1 were taken:

- Step 1. forming the required database of the operational EO-satellites;
- Step 2. selecting the mission phases and associated control modes;
- Step 3. selecting the critical PRs and their quantitative criteria;
- Step 4. specifying the performance constraints and their quantitative criteria;
- Step 5. determination of the system DPs;
- Step 6. identification of the system MDPs;
- Step 7. redefining the performance parameters based on the MDPs; and
- Step 8. (the most crucial step) comparing the outcome of the matching diagram to achieve the best point design in terms of performance.

2.2 Passive scan agile earth observation satellite attitude determination and control subsystem components

The ADCS performance sizing in this paper means size, weight and power (SWaP) (Wertz *et al.*, 2011), i.e. determining the size, weight (mass), and required consuming power of the subsystem based on PRs. For this purpose, its components including sensors and actuators (Zhang *et al.*, 2019) must be sized.

Sensors are generally selected as commercial of-the-shelf products based on technical specifications and considerations such as size, weight, spatial heritage, TRL, cost and reliability. Magnetic torquers (MT) are used to create control torques in the following mission phases and associated control modes:

- In the launch and early orbit phase (LEOP) – detumbling control mode to stop the rotation of the satellite around the I_{max} axis after separation; and
- In the normal phase to perform attitude maneuvers, to counteract the drifts caused by disturbance torques (Qi *et al.*, 2018; Wang *et al.*, 2018) and also to desaturate momentum-exchange elements (though they usually require much more time than thrusters).

So, MTs are sized based on the following requirements:

- The tumbling angular velocity around the I_{max} axis;
- The time interval required to detumble the EO-satellite;
- The worst-case disturbance torque; and
- The size of the used reaction wheels (RW).

Therefore, it can be concluded that the sizing of MTs should be done serially, not parallel and indeed after sizing the RWs.

2.3 Passive-scan agile earth observation satellites as design problem

Passive-scan agile earth observation satellites (PS-AEOS) are semi agile systems that have two-axis (roll and pitch) attitude maneuvering capabilities. Passive scan imaging mode means the satellite keeps a fixed attitude during the imaging process, and thus, the imaging direction is always parallel to the ground track (Yang *et al.*, 2018). The success of such a satellite mission depends on providing the best quality and most on-time image data to the users. Therefore, effective attitude determination and control is a vital part of this type of EO-satellites. Such a satellite with the PRs, constraints and mission specifications illustrated in Table 1 has been selected as a case. The design problem is to size a custom ADCS for this operational EO-satellite.

It is assumed that the EO-satellite IPL is rigidly connected to the platform without any interface mechanism, so its pointing and retargeting is performed only through the platform slew. Therefore, ADCS is solely responsible for the whole of geolocation or system pointing errors.

3. Constructing the attitude determination and control subsystem matching diagram

3.1 Database members

EO-satellites are divided into four categories including VHR (GSD $\leq$ 1 m), HR (1 $<$ GSD $\leq$ 4 m), MR (4 $<$ GSD $\leq$ 30 m) and LR (GSD $>$ 30 m) based on their Spatial resolution (Hwang, 2013).

We have examined the total number of 50 EO-satellites (Kramer, 2002), which 36 of them fall in very high resolution (VHR) and the remaining 14 falls in high resolution (HR) category. Their manufacturing technology was up to date and in the same level.

3.2 The performance phases and functional modes

The study also reveals that there are particular performance phases and functional modes of ADCS that could be categorized in specific tables such as Table 2.

During the mission entire time, the EO-satellites must be in one of the control modes.

Figure 1 Stepwise approach taken for the matching diagram construction

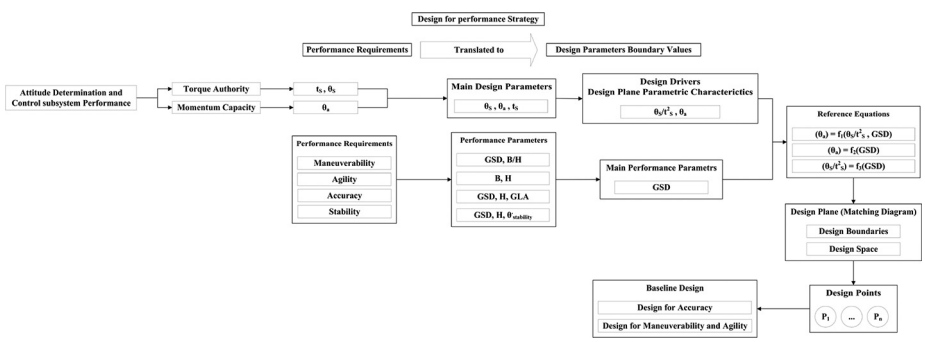

Table 1 PRs, constraints and mission specifications

Parameter	Value
Satellite mass	100 ± 15 Kg
Satellite mission	Remote sensing
No. of imaging sensors	2
Spatial resolution	1 m
Orbital altitude	500 ± 50 Km (near-circular orbit)
Orbital period	5677 ± 62 s
Orbital inclination angle	55 ± 1 deg
Satellite life-cycle	2 years
ADCS maximum mass	10 Kg
ADCS maximum consuming power	32 W

3.3 Critical performance requirements

The most critical PRs are often imposed on ADCS by the other subsystems of EO-satellites (Wertz *et al.*, 2011). These system requirements, which also identified as intermediate requirements could be divided into five categories including maneuverability, agility, accuracy, stability and durability and could be defined as follows:

1 Maneuverability: to turn as much as needed.
2 Agility: to maneuver as fast as needed.
3 Accuracy: to point to the required target with the minimum deviation (control)/to estimate the pointing direction with minimum error (knowledge).
4 Stability: to remain in a bounded domain around pointing direction with minimum jitter or random motion.
5 Durability: to fulfill as long as the mission life.

The study shows the ADCS performance, effects directly on the outcome of an EO-mission; therefore, the PRs of the ADCS are mostly affected by the image and also the IPL PRs.

3.3.1 Maneuverability.

As just stereo and natural hazards images are acquired by attitude maneuvers to point the targets located in off-nadir of the satellite so this top-level PR is mostly considered in single-pass stereo imaging and natural hazards imaging and not in continuous strip monoscopic imaging mode (Sun *et al.*, 2019; Yu and Wang, 2019; Zhang *et al.*, 2019).

Stereo images are acquired after running the slew maneuvers in along-track directions (Hirano *et al.*, 2003). The stereo pairs could be acquired from zenith, forward and/or backward point of the target area. According to equation (1), θ_s (slew angle) could be written as a function of B and H as follows:

$$\theta_s(B,H) = 90 - \tan^{-1}\left[\frac{\sqrt{(R_E+H)^2 - (B/2)^2} - R}{(B/2)}\right] - \sin^{-1}\left[\frac{(B/2)}{R_E+H}\right] \quad (1)$$

θ_s could be approximated by equation (2) as a function of Base (B) to Height (H) ratio, B/H, which is a decisive factor for achieving high precision images (Lemmens, 1392).

$$\theta_s(B/H) = tan^{-1}(B/H) \quad (2)$$

Although B/H can take different values from 0 to 1 and even more than 1, the ideal value for the B/H ratio to digital elevation model (DEM) production from stereo pairs is 0.6 (Hirano et al., 2003).

The relation equation (3) analytically exists between the pixel size in off-nadir ($GSD_{off-nadir}$) with pixel size in nadir point (GSD_{nadir}) of the IPL.

$$GSD_{off-nadir} = GSD_{nadir}\frac{\sqrt{B^2+H^2}}{H} sec\left[tan^{-1}\left(B/H\right)\right] \quad (3)$$

Equation (4) indicates that θ_s is also a function of Spatial resolution.

$$\frac{GSD_{off-nadir}}{GSD_{nadir}} = \frac{H^2+B^2}{H^2} sec^2\left[\tan^{-1}\left(\frac{B}{H}\right)\right] = \sec^2(\theta_s) \quad (4)$$

Because of the processing limitations, the pixel elongation due to the slew maneuvers cannot exceed 40% (Saghari *et al.*, 2018). For pixel size ratio of 1.4, B/H equals to 0.6 and the constraint $\theta_S \leq 30°$, could be considered for the slew angle.

The attitude maneuvers in natural hazards imaging mode run in the cross-track direction to reduce the EO-satellite revisit time of the target area. The slew angle, θ_s could be written as a function of H as follows:

Table 2 The performance phases of EO-satellites and the associated functional modes of ADCS

	Performance phases					
	Prelaunch	**LEOP**	**Commissioning**	**Orbital maneuvering**	**Normal**	**Deorbit**
Control modes						
Off	✓	✓	✓	✓	✓	✓
Idle	–	✓	✓	✓	✓	✓
Diagnostic	–	✓	✓	✓	✓	✓
Detumbling	–	✓	✓	✓	✓	✓
Coarse pointing	–	✓	✓	✓	✓	–
Safe	–	✓	✓	✓	✓	✓
Sun pointing	–	✓	✓	✓	✓	–
Fine pointing	–	–	–	✓	✓	–

Note: ✓ :active mode

$$\theta_s(H) = SIN^{-1}\left(\frac{R_E}{R_E + H}\right) \quad (5)$$

3.3.2 Agility

Attitude maneuvers are associated with time constraints. Therefore, every EO-satellite should be agile enough to carry out its mission correctly. The minimum available time, t_s, for retargeting as much as θ_s equation (2) could be calculated from equation (6) as a function of B and H as follows:

$$t_s(B,H) = 2\sqrt{\frac{(R_E + H)^3}{\mu}}\sin^{-1}\left(\frac{B}{2(R_E + H)}\right)[s] \quad (6)$$

3.3.3 Accuracy

The accuracy requirement in ADCS performance sizing of EO-missions could be categorized into attitude knowledge and pointing accuracy (KA, PA). These types of accuracy contribute, respectively, to the image localization and location.

KA represents the ADCS error in estimating the IPL pointing direction during the imaging mode. The KA is chosen in a way to support the geolocation accuracy (GLA) (Kramer, 2002); therefore, it could be considered as a function of GLA.

GLA is the difference between ground surveyed and imagery derived ground coordinates and could be considered as a criterion for meeting the ADCS PRs (Li and Xu, 2018). GLA is expressed in relative and absolute terms (R-GLA and A-GLA) (Kramer, 2002) that, in the following, GLA means A-GLA and is equal to "raw image location error".

As illustrated in equation (7), KA can be written as a function of GLA and orbit altitude, H as follows:

$$KA(H, GLA) = tan^{-1}\left({}^{GLA}/_{H}\right) \quad (7)$$

According to the statistical data, GLA and ground sample distance (GSD) have a competing nature correlation as illustrated in Figure 2. In EO-satellites with the same spatial resolution output, GLA output is lower in which has been designed and manufactured recently.

Figure 2 Changes of GLA to GSD in the USA made EO-satellites

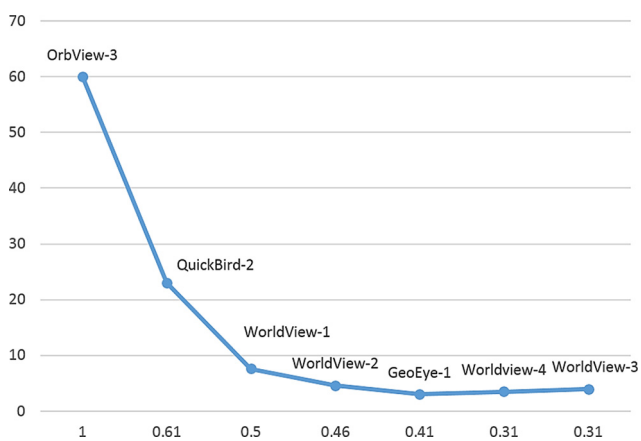

Empirically, GLA is considered 30 times of GSD but using statistical data, GLA could be written as a function of GSD as follows:

$$GLA(GSD) = -1989GSD^4 + 4104GSD^3 - 2701GSD^2 + 710.9GSD - 60.83 \quad (8)$$

Equation (8) is extracted by the Matlab curve fitting tool. The fit goodness criteria are listed in Table 3.

PA is the determinant of platform accuracy in pointing to the target area in the imaging mode. PA is driven by KA and empirically considered to be 10 times of that.

3.3.4 Stability

The "platform attitude stability" during imaging mode is another PR of EO-satellites ADCS and contributes to image quality. For an EO-mission, during the dwell time, the drift of the satellite shall be less than 20% of the instant field of view (IFOV) resulting in a drift rate that could be considered equal to required stability (Sandau, 2004). For EO-satellites in circular orbits, the stability could be written as a function of H and GSD as illustrated in equation (9).

$$\theta_{stability}(GSD, H) = \frac{0.4}{GSD} \times \frac{\tan^{-1}\left({}^{GSD}/_{2H}\right)}{\sqrt{{}^{(R_E + H)}/_{\mu}}}[deg/s] \quad (9)$$

3.4 Critical performance constraints

The attitude determination and control capability of EO-satellites is limited by having small budgets for mass and power. Although such limitations are not performance constraints, they are system constraints, which dominate the ADCS design as follows:

- The maximum mass of the ADCS (m_{ADCS}) is about 6% of the satellite dry mass.
- The maximum consuming power (P_{ADCS}) is about 12% of the satellite total power.
- After performance sizing, the results can be verified considering the above constraints.

3.5 System main design parameters

In sizing wheels always two performance quantities are considered, namely, angular momentum capacity and torque authority. The slew torque for RWs could be calculated by equation (10), in which I_S is the EO-satellite moment of inertia about slew axis, θ_{max-s} is the maximum needed slew angle and t_{min-s} is the minimum time for slew to be done during it (Wertz *et al.*, 2011).

$$T = (4I_S)(\theta_{max-S}/t^2_{min-S}) \quad (10)$$

Table 3 The validation of fit goodness

Equation no.	SSE	R^2	RMSE
(9)	0.133	0.9999	0.2578

The momentum capacity will be calculated by equation (11), in which T_D is the worst-case anticipated disturbance torque, θ_a is the PA and P is the orbital period.

$$h = (T_D)(1/\theta_a) \cdot (P/4) \tag{11}$$

Therefore, the parameters θ_{max-S}, t_{min-S} and θ_a, which appeared earlier in equations (2) (6) and (7) also appeared again in equations (10) and (11). These parameters are considered as the MDPs of ADCS and their categories (Ahmadi *et al.*, 2018), as well as the critical PRs, are given in Table 4.

3.6 Design drivers and parametric characteristics of the matching diagram

The matching diagram is a two-dimensional space, but according to Table 4, there are three MDPs that should be combined to form the design drivers, which determine the parametric characteristics of EO-satellites' ADCS matching diagram.

As $\theta_{max-S}/t^2_{min-S}$ and $1/\theta_a$ have appeared in equations (10) and (11), the design drivers could be $\theta_{max-S}/t^2_{min-S}$ and θ_a as the first choice. $\theta_{max-S}/t^2_{min-S}$ represents satellite maneuverability and agility and θ_a represents image location accuracy.

According to Step 3.3, both design drivers are functions of GSD. Therefore, the standard form of the ADCS reference equations should be as illustrated in equation (12).

$$\begin{cases} \theta_a = f_1\left({}^{\theta_S}/_{t_s^2}, GSD\right) \\ \theta_a = f_2(GSD) \\ {}^{\theta_S}/_{t_s^2} = f_3(GSD) \end{cases} \tag{12}$$

3.7 Matching diagram, point designs and baseline design

Using the reference equation (12), the matching diagram can be formed in a way that its vertical axis is θ_a and its horizontal axis is θ_S/t_s^2. Equation (13) has been extracted statistically as follows:

$$\begin{cases} \theta_a = 0.07715 - 0.1755GSD - 5.538\,{}^{\theta_S}/_{t_s^2} + 0.1111GSD^2 + 5.614GSD.\,{}^{\theta_S}/_{t_s^2} + 114.3\left({}^{\theta_S}/_{t_s^2}\right)^2 \\ \theta_a = 0.07972GSD^{2.144} - 0.005682 \\ {}^{\theta_S}/_{t_s^2} = \dfrac{0.01934GSD^2 - 0.01779GSD + 0.004122}{GSD^2 - 0.9719GSD + 0.239} \end{cases} \tag{13}$$

The quantitative criteria of fit goodness are listed in Table 5.

For different values of GSD from 0.7 to 1 m, the matching diagram can be drawn up as shown in Figure 3. The main functionality of the matching diagram is to integrate the design boundaries. The ADCS design boundaries for VHR PS-AEOSs with 1 m Spatial Resolution is illustrated in Figure 4.

Table 4 ADCS performance-critical requirements, MDPs, their category and brief descriptions

Performance critical requirements	DP	Category	Description
Maneuverability	θ_{max-S}	Energy	Maximum slew
Agility	t_{min-S}	Information	Minimum time needed to the max slew
Accuracy and Stability	θ_a	Matter	Yaw accuracy

Table 5 The validation of fit goodness

Equation no.	SSE	R^2	RMSE
(13-1)	1.0779e_07	1	3.2832e_4
(13-2)	1.3025e_04	0.9684	0.0057
(13-3)	6.2196e_6	0.9753	0.0018

For GSD = 1 m the "allowable design area" of the ADCS has a trapezoidal shape. All, the points in and on the boundaries of the design space are the "Point Designs" but the "baseline design points" are often on the boundaries. According to equations (10) and (11) to control the EO-satellite attitude with smaller actuators, the designers tend to select a point with the maximum θ_a and minimum θ_S/t^2.

In Figure 4, Points 1 and 2 could be considered as the "baseline design points," both of which are on the boundaries of the "allowable design area." If agility and maneuverability weigh more than accuracy (design for agility and maneuverability), then Point 1 and otherwise (design for accuracy) Point 2 could be selected as the baseline design. It is also possible to compare the calculation results for both points in terms of weight and power consumption. The baseline design points coordinates are (0.0228, 0.0739) for Point 1 and (0.0212, 0.0657) for Point 2.

The matching diagram as drawn up for PS-AEOSs with GSD = 1 m could be formed for other EO-satellites with different GSD values. Therefore, the design drivers θ_a and θ_S/t_s^2 could be determined subsequently.

4. Passive-scan agile earth observation satellite attitude determination and control subsystem performance sizing

In this section, the general procedure of performance sizing via the matching diagram technique is implemented for ADCS of a PS-AEOS, which introduced in Table 1 as a case.

Figure 3 Matching diagram for VHR EO-satellites (GSD $\leq$ 1 m)

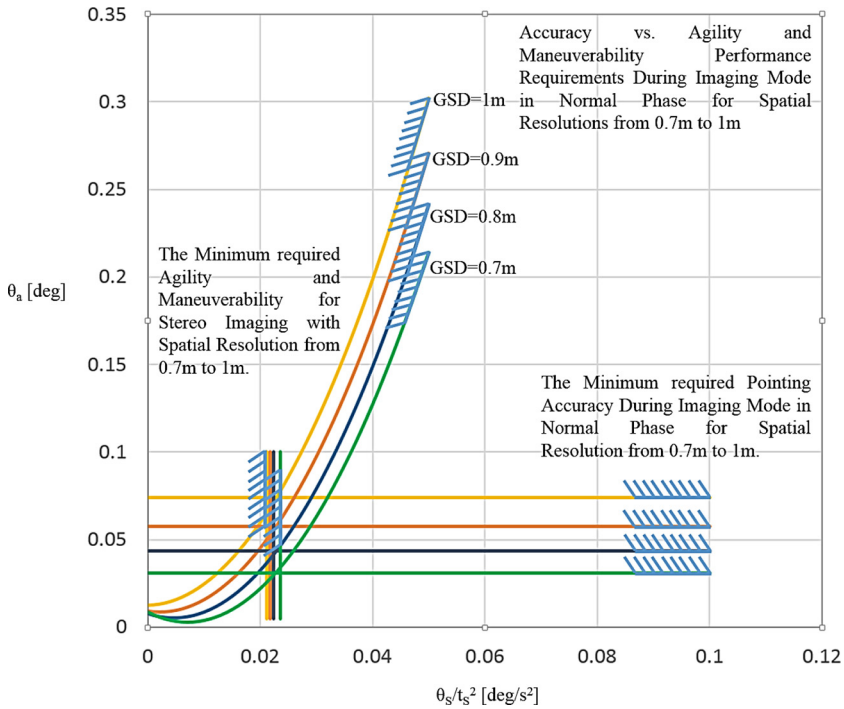

Figure 4 ADCS matching diagram, design boundaries, design space and design points for GSD = 1

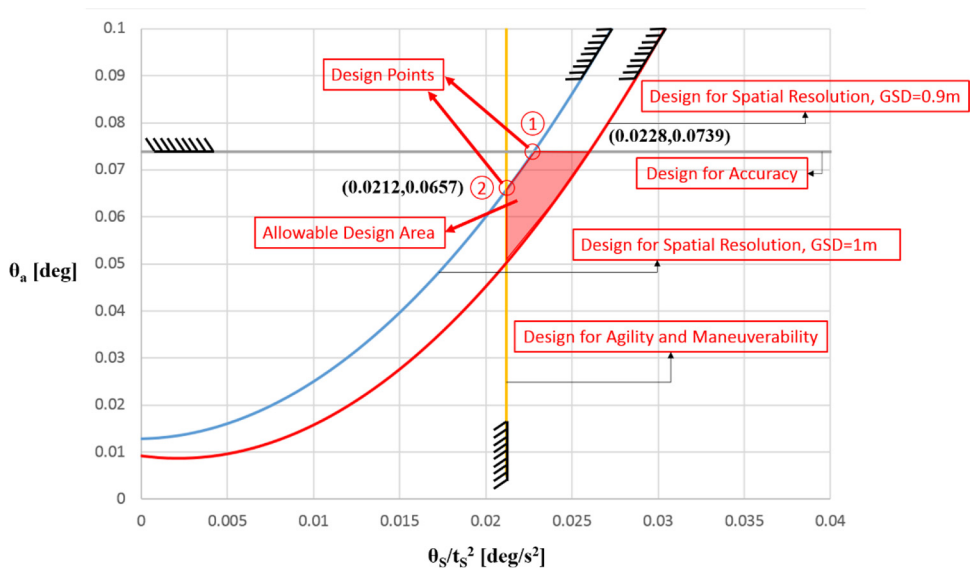

4.1 Performance phases and associated control modes

Besides Table 2, the intended EO-satellite has an additional performance mode called forward motion compensation (FMC). FMC mode will be activated during the imaging mode of the normal performance phase to raise the signal to noise ratio and the slew rate is 0.3 deg/s. The FMC mode slew rate is considered as a performance constraint.

4.2 Attitude control and stabilization method

A variety of stabilization and attitude control methods proper for AEOSs have been presented in (Wertz *et al.*, 2011). According to equation (8), the required GLA is 61.07 m so according to equation (7), KA and PA will be 0.007° and 0.07°, respectively. Therefore, the only applicable attitude control method is zero momentum bias (ZMB) stabilization (Wertz *et al.*, 2011).

Some other qualitative criteria were considered to have a comparative trade study among attitude control and stabilization methods. According to Table 6, the ZMB 3-axes stabilization method has the most functionalities to be applied in PS-AEOSs ADCS.

Table 6 Stabilization methods trade study based on qualitative criteria

Stabilization method	Three-axes stabilization	High pointing accuracy	Nadir pointing accuracy	Attitude maneuverability	Orbital maneuverability	Insensitivity to mass properties and unbalance	High stability	simplicity	Lifecycle duration
Gravity gradient									
Semi-passive	–	–	–	–	–	–	–	✓	✓
Semi-active	✓	–	✓	–	–	–	✓	✓	✓
Spin									
Normal-spin	–	–	–	–	✓	–	–	✓	✓
Dual-spin	–	–	–	–	✓	–	✓	–	✓
Three-axes									
Momentum-bias	✓	–	–	–	✓	✓	✓	–	✓
ZMB	✓	✓	✓	✓	✓	✓	✓	–	✓

4.3 The best sensor/actuator suite

The ADCS components, which are applicable in the sample PS-AEOS will be determined based on calculated KA and PA. The graph illustrated in (Graven *et al.*, 2008) or the table presented in (Jaafar Salehi *et al.*, 1393) provides such a tool to choose a proper suite of attitude determination sensors (ADS) and attitude control actuators (ACAs). Using these tools, the product tree can be drawn up as shown in Figure 5.

The sample PS-AEOS ADCS has been equipped with reserve components based on the principle of redundancy to avoid single-point failure. In each control mode, just a sub-suite of sensors and actuators is active based on the required accuracy (Table 7).

4.4 Attitude determination sensors performance sizing

According to Figure 5, the proper ADSs for the sample PS-AEOS ADCS are angular velocity sensor, sun sensor and magnetic sensors, which their technical specifications are depicted in Tables 8 to 10.

Figure 5 Product tree of the sample EO-satellite ADCS

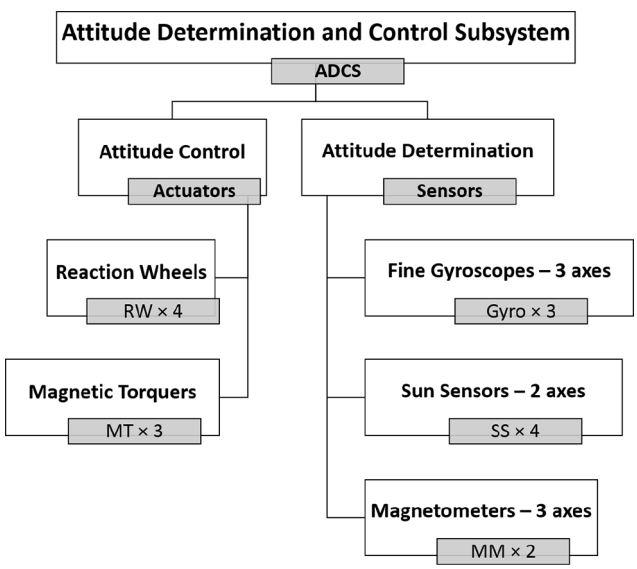

The total mass and consuming power of the ADSs suite are 0.36 Kg and 4.14 W, respectively.

4.5 Attitude control actuators performance sizing

According to Figure 5, other than thrusters, RWs and MTs will be used in the intended PS-AEOS ADCS. The performance sizing of ACAs is done based on two general approaches as follows:

1. To provide the required torques well above the peak disturbance torque – "accuracy" PR.
2. To provide the required control torques to perform slew maneuvers – "agility" and "maneuverability" PRs.

The external torques which have been considered in the first approach were gravity gradient, earth magnetic field, solar flares and aerodynamics. Inaccuracy in the center of gravity, misalignment of the thrusters, non-matching the output of the thrusters, rotary motors, viscosity of the liquids, flexible body dynamics and thermal shocks on flexible joints were the considered internal torques.

4.5.1 Reaction wheels

According to equations (10) and (11), for platform "maneuverability" and "agility," RWs' "torque capability" is equal to 13.8 mNm and for platform "accuracy," their "momentum capacity" is 0.345 Nms.

After reviewing some models of wheels, which are applicable in the sample EO-satellite, WHL wheels manufactured by JAXA has been selected and the complete technical specifications are listed in Table 10. Adding brackets, the mass of these wheels will increase by up to 25%.

4.5.2 Magnetic torquers

The MTs are sized based on PRs in LEOP detumbling mode. Torque capability in this mode is calculated by equation (14).

$$T = I\alpha = I\Delta\omega/\Delta t \tag{14}$$

In the absence of more limited data, the typical tumbling rate after separation could be specified as $\Delta\omega = 10\sqrt{3}$ deg/s and it is expected to be de-tumbled after two orbital periods so Δt = 11,354 s. The de-tumbling torque capability is equal to

Table 7 Stim210 Gyro sensor technical specifications

Model	Manufacturer	No. of axes	Bias stability (deg/hr)	Angle random walk (deg/1/2 h)	Mass (Kg)	Power (W)	Interface
Stim210	Sensonor	Tri-axes	0.5	0.15	0.052	1.5	RS422

Table 8 SS411 Sun sensor technical specifications

Model	Manufacturer	Accuracy (deg)	Mass (Kg)	Consuming power (W)	Interface
SS411	Sinclair interplanetary	0.1	0.034	0.135	UART, SPI, I2C, CAN or RS485

Table 9 The AMR magnetometer technical specification

Models	Manufacturer	Resolution (nT)	Mass (Kg)	Power (W)	Interface	Space heritage
AMR	ZARM	10	0.06	0.3	RS422	✓

Table 10 WHL wheel specifications

Model	Manufacturer	Produced torque (mNm)	Angular momentum (Nms)	Mass (Kg)	Power consumption @nominal angular velocity (W)
WHL	JAXA	15	0.4	1.2	5

Table 11 MT15-1 MT technical specifications, mass and consuming power

Models	Manufacturer	Magnetic moment ($A.m^2$)	Mass (Kg)	Power (W)
MT15-1	ZARM	15	0.43	1.11

1.5×10^{-3} Nm and the magnetic moment of the MTs is equal to 30 $A.m^2$ (Wertz and Larson, 2005).

Some models of applicable MTs were reviewed and according to technical specifications of the available variants, the required torque for each axis (roll, pitch and yaw) should be provided using two MTs, so the magnetic moment of each MT should be 15 $A.m^2$. Therefore, MT15-1 manufactured by ZARM has been selected whose technical specifications are listed in Table 11.

The total mass and consuming power of the sample EO-satellite ACAs are 7.8 Kg and 26 W, respectively. The total mass and consuming power of the intended satellite ADCS sensors/actuators suite are 8.16 Kg and 30.14 W, respectively.

According to the sample satellite system commodity budget, the total mass of ADCS must be less than 10 Kg and the total consuming power must be less than 32 W. For the first class of generational maturity (Rioux, 2005), at the proposal stage of small satellites, the maximum mass and power contingencies could be 35% and 80%, respectively. ADCS of the intended PS-AEOS has been sized with an 18% error in mass and 6% error in consuming power, which both of them are in the allowable margin.

5. Conclusion

This paper presents a rapid method for performance sizing of EO-satellites ADCS, using a matching diagram technique that is well-known in aircraft industries for aircraft design.

In the proposed method, the system requirements imposed by the imaging payload, power supply, communications and thermal control subsystems have been divided into five categories of higher-level requirements among, which maneuverability, agility and accuracy have been identified as the critical PRs. Due to the type of mission discussed in this paper, spatial and temporal resolutions have been considered as the top-level PRs. Maximum mass and consuming power are also considered as critical system constraints.

"Yaw accuracy-θ_a," "maximum slew angle-θ_S" and the "minimum available time for slewing to θ_S," which is indicated by t_S have been identified as the MDPs of ADCS. The design drivers were defined as θ_a and θ_S/t_S^2 according to the equations governing the sizing process. These equations aided the design boundaries to be drawn up and integrated to form the design space. Potentially all the design points in the design space could be selected as the point design, but the best point should have the maximum value of θ_a and the minimum value of θ_S/t_S^2. Therefore, the baseline design was selected on the boundary of the allowable design area with only two iterations.

To verify the results and validate the developed matching diagram, the ADCS of an operational PS-AEOS were sized based on performance, using the established design technique. The results were verified for the following reasons. First, the total mass and power consumption was 8.16 Kg (18% error) and 30.14 W (6% error), which, none of them violate the respective constraints. Secondly, the GLA in the sample EO-satellite is predicted to be less than 100 m.

In this paper, we applied the matching diagram technique for ADCS performance sizing, but the research is aimed to be continued for the entire EO-satellite system.

References

Ahmadi, A., Kosari, A. and Malaek, S.M.B. (2018), "A generic method for remote sensing satellites conceptual design and rapid sizing based on design for performance strategy", *IEEE aerospace & electronics systems magazine*, Vol. 33 No. 2, pp. 34-51.

Akbaritabar, S., Esmaelzadeh, R. and Zardashti, R. (2018), "Comparing fluid ring and CMG servomechanisms for active control of rigid satellites", *Aircraft Engineering and Aerospace Technology*, Vol. 90 No. 6, pp. 896-905.

Graven, P., Plam, Y., Hansen, L.J. and Harvey, S. (2008), "Implementing plug-and-play concepts in the development of an attitude determination and control system to support operationally responsive space", in *IEEE Aerospace Conference, Big Sky, MT, USA*.

Hirano, A., Welch, R. and Lang, H. (2003), "Mapping from ASTER stereo image data: DEM validation and accuracy assessment", *ISPRS Journal of Photogrammetry & Remote Sensing*, Vol. 57 Nos 5/6, pp. 356-370.

Hua, S., Huang, H., Yin, F. and Wei, C. (2018), "Constant-gain EKF algorithm for satellite attitude determination systems", *Aircraft Engineering and Aerospace Technology*, Vol. 90 No. 8, pp. 1259-1271.

Hwang, F.T. (2013), *Current Development Status and Future Trends for high-resolution optical earth observation satellites*, in Asian Association on Remote Sensing, Bali, Indonesia.

Jaafar Salehi, A., Mirshams, M. and Saghari, A. (1393), "Comperehensive conceptual design code for remote sensing satellites", *JSST*, Vol. 7 No. 2, pp. 35-47.

Jia, Q., Li, H., Chen, X. and Zhang, Y. (2019), "Observer-based reaction wheel fault reconstruction for spacecraft attitude control systems", *Aircraft Engineering and Aerospace Technology*, Vol. 91 No. 10, pp. 1268-1277.

Kramer, H.J. (2002), *Observation of the Earth And its Environment: A Survey of Missions And Sensors*, Berlin Heidelberg: Springer-Verlag.

Kwiek, A. (2019), "Conceptual design of an aircraft for Mars mission", *Aircraft Engineering and Aerospace Technology*, Vol. 91 No. 6, pp. 886-892.

Laurence, J. and Loftin, K. (1980), *Subsonic aircraft: evolution and the matching of size to performance*, Hampton, VT: NASA,

Lemmens, M. (1392), "High-resolution 3-D images", *Cartography Journal (In Persian)*, No. 114, pp. 21-23.

Li, M. and Xu, B. (2018), "Autonomous orbit and attitude determination for Earth satellites using images of regular-shaped ground objects", *Aerospace Science and Technology*, Vol. 80, pp. 192-202.

Li, H. Duan, L. Liu, X. and Cai, G. (2017), "Deployment and control of cable-driven flexible solar arrays," *Aircraft Engineering and Aerospace Technology*, vol. 89, no. Please can you request that a new special issue slot is added into scholar one for JIC and request that the special issue "Intellectual Capital and Corporate Environmentalism" is set up in this place with Gregorio Martín-de Castro as the lead guest editor", 6, pp. 835-844.

Malaek, S.M.B., Mollajan, A., Ghorbani, A. and Sharahi, A. (2015), "A new systems engineering model based on the principles of axiomatic design", *Journal of Industrial and Intelligent Information*, Vol. 3 No. 2, pp. 143-151.

Palacios, E.S. and Smith, H. (2019), "Impact of mission requirements on the design of low observable UCAV configurations", *Aircraft Engineering and Aerospace Technology*, Vol. 91 No. 10, pp. 1295-1307.

Qi, N. m., Sun, Q. and Yang, Y. (2018), "Effect of J3 perturbation on satellite position in LEO", *Aircraft Engineering and Aerospace Technology*, Vol. 90 No. 1, pp. 74-86.

Raymer, D.P. (1992), *Aircraft design: a conceptual approach*, United States of America: American Institute of Aeronautics and Astronautics, Inc.

Rioux, N. (2005), *ANSI/AIAA guide for estimating spacecraft systems contingencies applied to the NASA GLAST mission*, IEEE,

Roskam, J. (1985), *Airplane design – part I: preliminary sizing of airplanes*, Ottawa, KS: Roskam Aviation and Engineering Corporation.

Sadraey, M.H. (2013), *Aircraft design - a systems engineering approach*, Chennai, India: John Wiley & Sons, Ltd.

Saghari, A., Rahmani, S., Kosari, A. and Ebrahimi, M. (2018), "Wasted performance minimization of the multi-purpose mini-satellite platform for an EO mission using a dynamic simulation-based model", *Aerospace Science and Technology*, Vol. 73, pp. 61-77.

Sandau, R. (2004), "A metrics to support the design of small satellite-based high-resolution mapping systems", in *18th Annual AIAA/USU Conference on Small Satellites, Logan, UT*.

Sun, J., Wu, X., Zhang, S., Guo, F. and Song, T. (2018), "Adaptive robust control of coupled attitude and orbit for spacecraft with model uncertainties", *Aircraft Engineering and Aerospace Technology*, Vol. 90 No. 1, pp. 186-195.

Sun, C., Jia, L., Xi, B., Liu, J., Wang, L. and Weng, X. (2019), "Genetic diversity and association analyses of fruit traits with microsatellite ISSRs in Sapindus", *Journal of forestry research*, Vol. 30 No. 1, pp. 193-203.

Tayebi, J., Nikkhah, A.A. and Roshanian, J. (2017), "LQR/LQG attitude stabilization of an agile microsatellite with CMG", *Aircraft Engineering and Aerospace Technology*, Vol. 89 No. 2, pp. 290-296.

Torenbeek, E. (1976), *Synthesis of subsonic - an introduction to the preliminary design of subsonic general aviation and transport aircraft, with emphasis on layout, aerodynamic design, propulsion and performance*, Netherlands: Delft University Press.

Wang, Y., Zhong, R. and Xu, S. (2018), "Orbital perturbation due to orbit-attitude coupling near asteroids", *Aircraft Engineering and Aerospace Technology*, Vol. 90 No. 1, pp. 104-113.

Wassan, C.S. (2006), *System analysis, design, and development concepts, principles, and practices*, United States of America: John Wiley & Sons, Inc.

Wertz, J.R., Everett, D.F. and Puschell, J.J. (2011), *Space mission engineering: the new SMAD*, Hawthorne, CA: Microcosm Press.

Wertz, J.R. and Larson, W.R. (2005), *Space mission analysis and design*, 3rd ed., United States of America: Microcosm Press and Kluwer Academic Publishers.

Xie, Y., Liu, P. and Cai, G. (2018), "On-orbit frequency identification of spacecraft based on attitude maneuver data", *Aircraft Engineering and Aerospace Technology*, Vol. 90 No. 1, pp. 33-42.

Xiong, K. and Wei, C. (2017), "Multiple-model adaptive estimator for spacecraft attitude sensor calibration", *Aircraft Engineering and Aerospace Technology*, Vol. 89 No. 3, pp. 457-467.

Yang, W., Chen, Y., He, R., Chang, Z. and Chen, Y. (2018), "The bi-objective active-scan agile Earth observation satellite scheduling problem: modeling and solution approach", in *2018 IEEE Congress on Evolutionary Computation (CEC)*, *Rio de Janeiro, Brazil*.

Yu, Z. and Wang, W. (2019), "Learning DALTS for cross-modal retrieval", *CAAI Transactions on Intelligence Technology*, Vol. 4 No. 1, pp. 9-16.

Zhang, J., Zhai, Y. and Li, D. (2019), "Fuzzy decision implications: interpretation within fuzzy decision context", *CAAI Transactions on Intelligence Technology*, Vol. 4 No. 4, pp. 231-236.

Zhang, J., Yuan, J., Wang, W. and Wang, J. (2019), "Reachable domain of spacecraft with a single normal impulse", *Aircraft Engineering and Aerospace Technology*, Vol. 91 No. 7, pp. 977-986.

Corresponding author

Amirreza Kosari can be contacted at: kosari_a@ut.ac.ir